Acta Crystallographica Section F
Structural Biology and Crystallization Communications
ISSN 1744-3091

Purification, crystallization and crystallographic analysis of *Dictyostelium discoideum* phenylalanine hydroxylase in complex with dihydrobiopterin and Fe^{III}

Ningning Zhuang,[a,b,c] Kyung Hey Seo,[a,b,c] Cong Chen,[a,b,c] Hye-Lim Kim,[d] Young Shik Park[d] and Kon Ho Lee[b,c,e]*

[a]Division of Applied Life Science (BK21 Program), Gyeongsang National University, Jinju 660-701, Republic of Korea, [b]Plant Molecular Biology and Biotechnology Research Center, Gyeongsang National University, Jinju 660-701, Republic of Korea, [c]Environmental Biotechnology National Core Research Center (EB-NCRC), Gyeongsang National University, Jinju 660-701, Republic of Korea, [d]FIRST Rearch Group, School of Biological Sciences, Inje University, Kimhae 621-749, Republic of Korea, and [e]Department of Microbiology, School of Medicine, Gyeongsang National University, Jinju 660-751, Republic of Korea

Correspondence e-mail: lkh@gnu.ac.kr

Received 3 February 2010
Accepted 25 February 2010

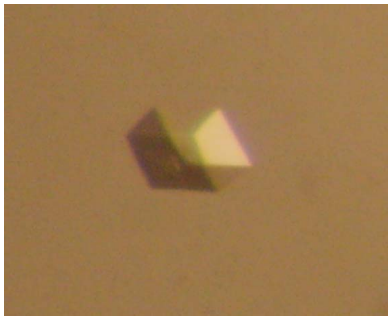

Dictyostelium discoideum phenylalanine hydroxylase (*Dic*PAH; residues 1–415) was expressed in *Escherichia coli* and purified for structural analysis. Apo *Dic*PAH and *Dic*PAH complexed with dihydrobiopterin (BH_2) and Fe^{III} were crystallized using 0.06 *M* PIPES pH 7.0, 26%(*w*/*v*) PEG 2000 by the hanging-drop vapour-diffusion method. Crystals of apo *Dic*PAH and the *Dic*PAH–BH_2–Fe^{III} complex diffracted to 2.6 and 2.07 Å resolution, respectively, and belonged to space group $P2_1$, with unit-cell parameters a = 70.02, b = 85.43, c = 74.86 Å, β = 110.12° and a = 70.97, b = 85.33, c = 74.89 Å, β = 110.23°, respectively. There were two molecules in the asymmetric unit. The structure of *Dic*PAH has been solved by molecular replacement.

1. Introduction

The nonhaem iron-dependent enzyme phenylalanine hydroxylase (PAH; EC 1.14.16.1) catalyzes the hydroxylation of the aromatic amino acid L-phenylalanine (L-Phe) to L-tyrosine (L-Tyr) in the presence of the specific cofactor tetrahydrobiopterin (BH_4) and dioxygen (O_2). As L-Tyr is the precursor of the neurotransmitter dopamine, the catabolism of L-Phe plays an essential role in the development of the neural system (Kaufman, 1993). Disorder of the PAH system leads to the diseases phenylketonuria and hyperphenylalaninaemia, which result in brain-development problems unless treated immediately after birth (Scriver & Kaufman, 1995). Full-length mammalian PAHs consist of three domains: an N-terminal regulatory domain, a central catalytic domain and a short C-terminal oligomerization domain for tetramer formation. The catalytic site includes a nonhaem Fe atom coordinated by a His-His-Glu catalytic triad that is highly conserved in aromatic amino-acid hydroxylases. Dysfunction of human PAH is mostly caused by mutations that are found in the catalytic domain. These mutations demonstrate different clinical, metabolic and enzymatic phenotypes (Erlandsen *et al.*, 2004). Crystallographic studies of human and rat PAHs revealed the binding sites of the pterin cofactor and the substrate, and provided insights into the substrate-specificity and catalytic mechanism of the enzyme (Erlandsen *et al.*, 1997; Fusetti *et al.*, 1998; Kobe *et al.*, 1999). Mammalian PAH responds with positive cooperativity to increased concentration of the substrate (Kaufman, 1993; Knappskog *et al.*, 1996).

There are four possible BH_4 stereoisomers: L-*erythro*-BH_4, L-*threo*-BH_4, D-*erythro*-BH_4 and D-*threo*-BH_4. L-*erythro*-BH_4 is ubiquitous in animals as the natural cofactor for aromatic amino-acid hydroxylases, whereas the social amoeba *Dictyostelium discoideum* produces both L-*erythro*-BH_4 and D-*threo*-BH_4 (DH_4; Klein *et al.*, 1990; Cho *et al.*, 1999). Interestingly, *Dictyostelium* PAH (*Dic*PAH) uses both as co-factors, although it exhibits higher activity with DH_4 than with L-*erythro*-BH_4 (Siltberg-Liberles *et al.*, 2008). This indicates that *Dic*PAH possesses dual cofactor specificity (Choi *et al.*, 2005). However, no structural information is available on the binding of DH_4 to PAH. In order to understand the enzyme-catalysis mechanism and dual cofactor specificity, *Dic*PAH (residues 1–415) was purified and crystallized for structural analysis. Three-dimensional structures of

*Dic*PAH will provide a deeper understanding of the cofactor specificity of the hydroxylase reaction and its regulatory properties.

2. Experimental

2.1. Protein expression and purification

*Dic*PAH (residues 1–415; *Dic*PAHΔ415) was cloned into the bacterial expression vector pProEx HTa (Life Technologies, Carlsbad, California, USA) to produce a recombinant protein with an N-terminal hexahistidine tag and a TEV protease cleavage site (MSYYHHHHHHDYDIPTTENLYFQG). *Escherichia coli* strain BL21 (DE3) was used for protein expression. 100 ml aliquots of an overnight culture were seeded into 1000 ml fresh Luria–Bertani (LB) medium (10 g Bacto tryptone, 5 g yeast extract, 10 g NaCl per litre of solution) containing ampicillin (100 µg ml^{-1}) at 310 K with vigorous shaking until the OD_{600} reached 0.6. Protein expression was induced for 5 h with 0.4 m*M* isopropyl β-D-1-thiogalactoside (IPTG) at 303 K and cells were harvested by centrifugation (6000 rev min^{-1}, 6 min, 277 K). The harvested cells were washed with phosphate-buffered saline (PBS; 8 g NaCl, 0.2 g KCl, 1.44 g NaH_2PO_4 per litre of solution; pH 7.4), resuspended in lysis buffer (50 m*M* sodium phosphate pH 7.4, 500 m*M* NaCl, 5 m*M* imidazole) and disrupted by sonication. After centrifugation (1 h at 12 000 rev min^{-1}) at 277 K, the clear supernatant was filtered (qualitative filter paper, Advantec, Japan) and loaded onto an open column of nickel–NTA beads (Qiagen, Hilden, Germany) pre-equilibrated with binding buffer. The column was washed first with ten column volumes of binding buffer and then with ten column volumes of washing buffer (50 m*M* sodium phosphate pH 7.4, 500 m*M* NaCl, 20 m*M* imidazole). The recombinant *Dic*PAHΔ415 was eluted with 50 m*M* Tris–HCl pH 8.0, 100 m*M* NaCl, 300 m*M* imidazole. Fractions containing *Dic*PAHΔ415 were pooled, concentrated and exchanged into 50 m*M* Tris–HCl pH 8.0, 1 m*M* EDTA by ultrafiltration (Centriprep YM-50, Millipore, Bedford, Massachusetts, USA). The N-terminal hexahistidine tag was then removed using 0.02 mg TEV protease (Invitrogen, Carlsbad, California, USA) per milligram of protein at 277 K overnight, leaving artifactual residues GAMDPEF at the N-terminus. After removal of the His tag, the *Dic*PAHΔ415 was further purified by anion-exchange chromatography on a Resource 15Q column (GE Healthcare, Piscataway, New Jersey, USA). The protein was eluted using a salt gradient and eluted at ∼200 m*M* NaCl pH 7.5. The fractions containing the *Dic*PAHΔ415 protein were finally purified by gel-filtration chromatography on a Superdex 200 column (GE Healthcare, Piscataway, New Jersey, USA) in 20 m*M* Tris–HCl pH 8.0, 150 m*M* NaCl. The *Dic*PAHΔ415 protein was pooled and concentrated to 10 mg ml^{-1} in 20 m*M* Tris–HCl pH 8.0 by ultrafiltration (Centricon YM-30, Millipore Corporation, Bedford, Massachusetts, USA) for crystallization. The protein purity was examined by SDS–PAGE and native PAGE. The protein concentration was determined using the Bradford assay (Bradford, 1976).

2.2. Crystallization and data collection

Crystallization of apo *Dic*PAHΔ415 was initially carried out using Crystal Screens I and II and Index Screen from Hampton Research (California, USA), Wizard Screens I and II and Cryo Screens I and II from Emerald BioStructures (Bainbridge Island, Washington, USA) and laboratory-made solutions using a microbatch crystallization method at 291 K. Drops containing equal volumes (1 µl) of protein solution (6 mg ml^{-1} in 20 m*M* Tris–HCl pH 8.0) and screening solution were equilibrated under Al's oil in a 72-well microbatch plate.

After crystals of apo *Dic*PAHΔ415 were produced from the initial screenings, further screenings to find optimal crystallization conditions were performed using hanging-drop vapour-diffusion trials, varying the pH range, type of precipitant, precipitant concentration and volume of the drop. To obtain crystals of the *Dic*PAHΔ415–BH_2 complex, BH_2 (the oxidized form of BH_4) was used as BH_4 is not stable under aerobic conditions. Apo *Dic*PAHΔ415 was incubated with 2 m*M* BH_2 (Fluka, Steinheim, Switzerland) for 1 h on ice prior to setting up crystallization. The *Dic*PAHΔ415–BH_2 complex crystals grew in the same condition as the apo *Dic*PAHΔ415 crystals. To incorporate Fe^{III} into the protein, the crystals of *Dic*PAHΔ415–BH_2 were soaked in well solution containing 5 m*M* $Fe(NH_4)_2(SO_4)_2$ (Sigma, Steinheim, Switzerland) for 1 h before flash-freezing. Crystals were flash-frozen in liquid nitrogen for data collection after soaking for 1 min in reservoir solution containing 12%(*v*/*v*) ethylene glycol. X-ray diffraction data were collected from apo *Dic*PAHΔ415

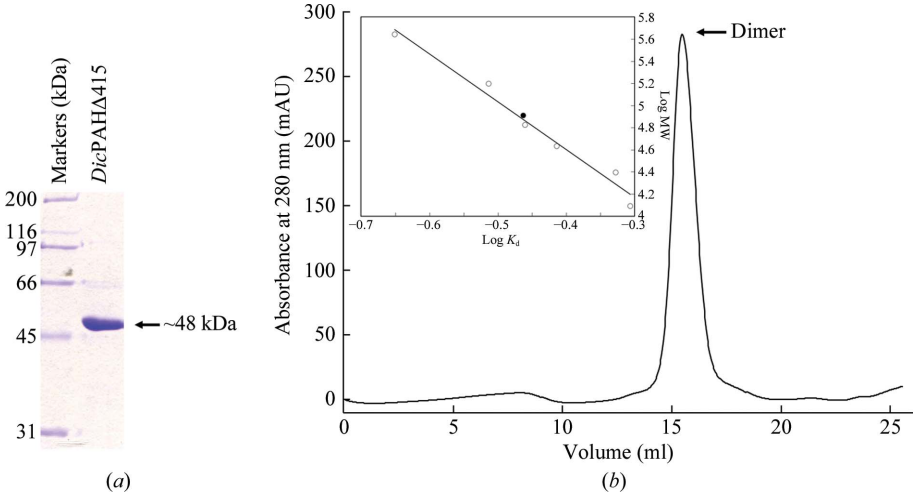

Figure 1
Purification of *Dic*PAHΔ415. (*a*) The purity of the *Dic*PAHΔ415 was confirmed by SDS–PAGE. (*b*) Analytical gel-filtration chromatography of *Dic*PAHΔ415. A single peak was observed that was estimated using protein standards to correspond to the size of a dimer. The inset shows logK_d against log(molecular weight) for protein standards (circles) and *Dic*PAHΔ415 (filled circle). K_d was calculated from the equation $K_d = (V_e - V_0)/(V_t - V_0)$, where V_e, V_t and V_0 represent the eluted volume, total volume and void volume, respectively. The standard proteins were ferritin (440 kDa), aldolase (158 kDa), BSA (67 kDa), ovalbumin (43 kDa), chymotrypsinogen A (25 kDa) and cytochrome *c* (12.4 kDa).

and *Dic*PAHΔ415–BH_2–Fe^{III} crystals using an ADSC Quantum 210 CCD detector with X-rays of wavelength 1.23985 Å on beamlines 4A and 6C1 of Pohang Accelerator Laboratory (PAL), Pohang, Republic of Korea, with exposure times of 30 s and 10 s for 1° oscillations at crystal-to-detector distances of 200 and 150 nm, respectively. All diffraction data were indexed, integrated and scaled using *HKL*-2000 (Otwinowski & Minor, 1997). Molecular replacement was performed using the program *AMoRe* (Collaborative Computational Project, Number 4, 1994; Navaza, 2001).

3. Results

Residues 1–415 of *D. discoideum* PAH (*Dic*PAHΔ415), corresponding to the N-terminal regulatory and central catalytic domains, were expressed in *E. coli* and purified for crystallization by nickel-affinity, ion-exchange and gel-filtration chromatography. The molecular weight of the protein was estimated to be about 48 kDa from SDS–PAGE, which is similar to the theoretical molecular weight of 47.5 kDa (Fig. 1*a*). The protein was separated by gel-filtration chromatography with an effective mass of 80 kDa, suggesting that the protein exists as a dimer in solution (Fig. 1*b*). From the initial crystallization trials, dendritic apo *Dic*PAHΔ415 crystals were found using the screening solution 0.1 *M* PIPES pH 6.5, 30%(*w*/*v*) PEG 4000 (Fig. 2*a*). Apo *Dic*PAHΔ415 crystals that were suitable for diffraction experiments were obtained by the hanging-drop vapour-diffusion method at 291 K in a drop containing 5 µl 6 mg ml^{-1} protein solution and 5 µl of a mixture of 9 µl reservoir solution [0.06 *M* PIPES pH 7.0, 26%(*w*/*v*) PEG 2000] and 1 µl 0.1 *M* L-proline as an additive. The crystals grew to maximum dimensions of 0.3 × 0.4 × 0.2 mm in 3–4 d (Figs. 2*b* and 2*c*). Data were collected to 2.6 Å resolution from a single crystal of apo *Dic*PAHΔ415 and were processed in the monoclinic space group $P2_1$, with unit-cell parameters $a = 70.02$, $b = 85.43$, $c = 74.86$ Å, $\beta = 110.12°$ (Table 1). *Dic*PAHΔ415–BH_2 complex crystals were obtained using the same condition as the apo *Dic*PAHΔ415 crystals and grew to maximum dimensions of 0.3 × 0.3 × 0.3 mm in 3–4 d (Fig. 2*d*). The crystals of the

Table 1
Data statistics for *Dic*PAHΔ415 crystals.

Values in parentheses are for the highest resolution shell.

	Apo *Dic*PAHΔ415	*Dic*PAHΔ415–BH_2–Fe^{III}
Resolution (Å)	50–2.60 (2.69–2.60)	50–2.07 (2.14–2.07)
Wavelength (Å)	1.23985	1.23985
Space group	$P2_1$	$P2_1$
Unit-cell parameters (Å, °)	$a = 70.02$, $b = 85.43$, $c = 74.86$, $\beta = 110.12$	$a = 70.97$, $b = 85.33$, $c = 74.89$, $\beta = 110.23$
No. of molecules per ASU	2	2
V_M ($Å^3$ Da^{-1})	2.24	2.24
Solvent content (%)	45.23	45.11
Unique reflections	25829 (2516)	50608 (4958)
Completeness (%)	99.2 (98.4)	99.1 (97.8)
Multiplicity	3.8 (3.8)	3.8 (3.7)
$\langle I/\sigma(I)\rangle$	26.3 (27.3)	9.3 (9.9)
R_{merge}† (%)	5.5 (9.8)	6.7 (59.8)

† $R_{merge} = \sum_{hkl}\sum_i |I_i(hkl) - \langle I(hkl)\rangle| / \sum_{hkl}\sum_i I_i(hkl)$, where $I_i(hkl)$ is the ith intensity measurement of reflection hkl, including symmetry-related reflections, and $\langle I(hkl)\rangle$ is its average.

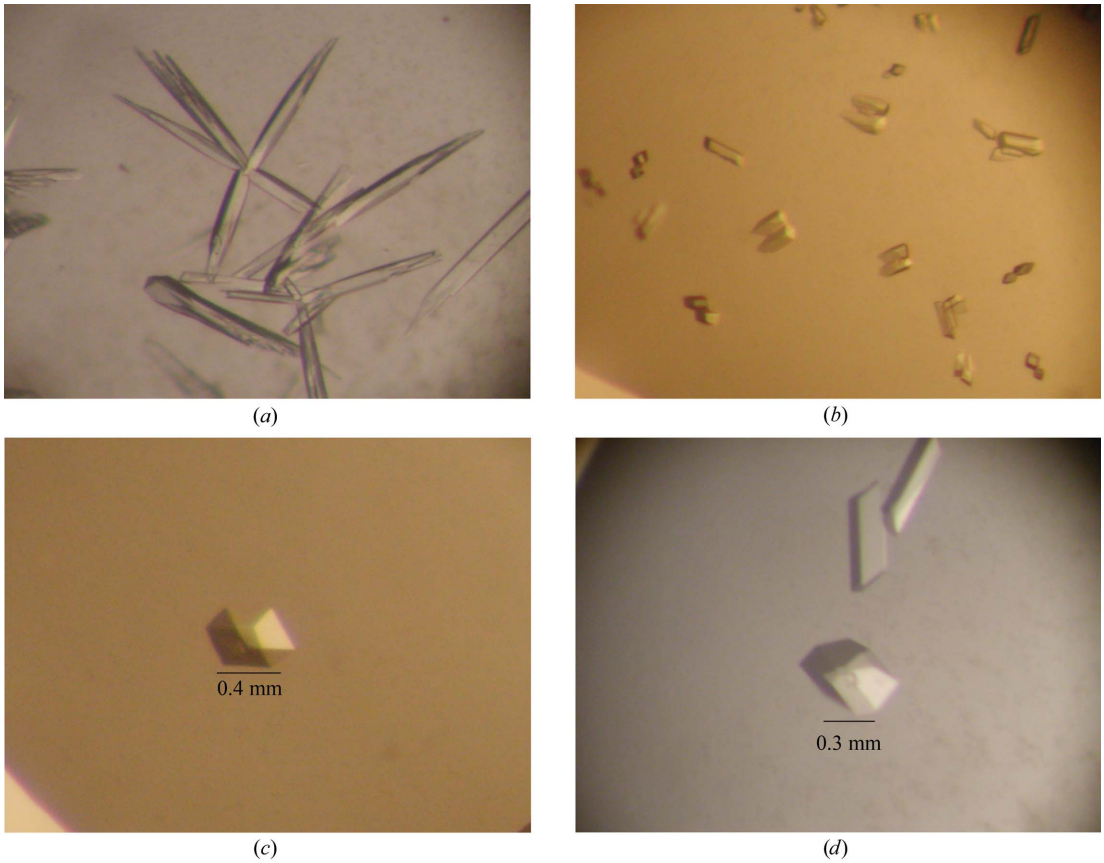

(*a*) (*b*) (*c*) (*d*)

Figure 2
Crystals of *Dic*PAHΔ415. (*a*) Dendritic crystals obtained from initial screening. (*b*) Overlapping rod-shaped crystals obtained after optimization. (*c*) The best large single crystal of apo *Dic*PAHΔ415 obtained after additive screening and controlling the drop size. (*d*) The best large single crystal complexed with BH_2 used for soaking with Fe^{III} and diffraction.

*Dic*PAHΔ415–BH_2–Fe^{III} complex were produced by soaking the *Dic*PAHΔ415–BH_2 complex crystals. The *Dic*PAH–BH_2–Fe^{III} complex crystal diffracted to 2.07 Å resolution and belonged to space group $P2_1$, with unit-cell parameters a = 70.97, b = 85.33, c = 74.89 Å, β = 110.23° (Table 1). For both crystal forms it was clear that higher resolution data were available and we plan to collect these data as soon as possible. The asymmetric unit contained two *Dic*PAHΔ415 molecules, with a Matthews coefficient V_M of 2.24 $Å^3$ Da^{-1} and an estimated solvent content of 45.23% (Matthews, 1968). The crystal of the *Dic*PAHΔ415–BH2–Fe^{III} complex had essentially the same Matthews coefficient and therefore the same number of molecules in the asymmetric unit and the same percentage solvent content. The structure of *Dic*PAHΔ415 could be determined by molecular replacement using the program *AMoRe* (Collaborative Computational Project, Number 4, 1994; Navaza, 2001). The human PAH catalytic domain (PDB code 1j8u; Andersen *et al.*, 2001) was used as a search model for molecular replacement, as it shares 64% amino-acid sequence identity in the catalytic domain. After a rotation and translation search, a solution consisting of two catalytic domains with a correlation coefficient of 33.3 and an R factor of 52.2% could be found and was refined to a correlation coefficient of 53.8 and an R factor of 45.7% using the fitting function in *AMoRe*. The missing N-terminal regulatory domain could be built into the electron densities calculated from the molecular-replacement solution (data not shown). Detailed discussion of the refined structures of both crystals will be published elsewhere.

We thank Dr H. S. Lee and the staff of beamlines 4A and 6B of Pohang Accelerator Laboratory for help with data collection. This work was supported by NRF grant 03-2009-0259 (KHL), NRF 313-2008-2-C00533 (YSP), grant No. 20090091494 from the MEST/NRF to EB-NCRC (KHL) and the BK21 program (NNZ, KHS and CC).

References

Andersen, O. A., Flatmark, T. & Hough, E. (2001). *J. Mol. Biol.* **314**, 279–291.
Bradford, M. M. (1976). *Anal. Biochem.* **72**, 248–254.
Cho, S. H., Na, J. U., Youn, H. Y., Hwang, C. S., Lee, C. H. & Kang, S. O. (1999). *Biochem. J.* **340**, 497–503.
Choi, Y. K., Park, J. S., Kong, J. S., Morio, T. & Park, Y. S. (2005). *FEBS Lett.* **579**, 3085–3089.
Collaborative Computational Project, Number 4 (1994). *Acta Cryst.* D**50**, 760–763.
Erlandsen, H., Fusetti, F., Martines, A., Hough, E., Flatmark, T. & Stevens, R. C. (1997). *Nature Struct. Biol.* **4**, 995–1000.
Erlandsen, H., Pey, A. L., Gámez, A., Pérez, B., Desviat, L. R., Aguado, C., Koch, R., Surendran, S., Tyring, S., Matalon, R., Scriver, C. R., Ugarte, M. & Stevens, R. C. (2004). *Proc. Natl Acad. Sci. USA*, **101**, 16903–16908.
Fusetti, R., Erlandsen, H., Flatmark, T. & Stevens, R. C. (1998). *J. Biol. Chem.* **273**, 16962–16967.
Kaufman, S. (1993). *Adv. Enzymol. Relat. Areas Mol. Biol.* **67**, 77–264.
Klein, R., Thiery, R. & Tatischeff, I. (1990). *Eur. J. Biochem.* **187**, 665–669.
Knappskog, P. M., Flatmark, T., Aarden, J. M., Haavik, J. & Martinez, A. (1996). *Eur. J. Biochem.* **242**, 813–821.
Kobe, B., Jennings, I. G., House, C. M, Michell, B. J., Goodwill, K. E., Sanatarsiero, B. D., Stevens, R. C., Cotton, R. G. H. & Kemp, B. E. (1999). *Nature Struct. Biol.* **6**, 442–448.
Matthews, B. W. (1968). *J. Mol. Biol.* **33**, 491–497.
Navaza, J. (2001). *Acta Cryst.* D**57**, 1367–1372.
Otwinowski, Z. & Minor, W. (1997). *Methods Enzymol.* **276**, 307–326.
Scriver, C. R. & Kaufman, S. (1995). *The Metabolic and Molecular Bases of Inherited Disease*, 8th ed., pp. 1667–1724. New York: McGraw–Hill.
Siltberg-Liberles, J., Steen, I. H., Svebak, R. M. & Martinez, A. (2008). *Gene*, **427**, 86–92.